Proceedings of ISFOG 2025
5TH INTERNATIONAL SYMPOSIUM ON
FRONTIERS IN OFFSHORE GEOTECHNICS
Nantes, France | June 9-13 2025

ISBN 978-2-85782-758-0

The effect of soil type and drainage conditions on cone penetration resistance in two-layered soil profiles

Y. Tian*
Fugro Belgium S.R.L., Louvain-la-Neuve, Belgium
Formerly University of Western Australia, Crawley, Australia

A. Arafianto, B. M. Lehane
The University of Western Australia, Crawley, Australia

**Y.tian@fugro.com (corresponding author)*

ABSTRACT: This paper investigates the influence of soil type and drainage conditions on the end resistance developed by a cone penetrometer installed in two-layered soil profiles. The investigation involved physical modelling in a calibration chamber and finite element simulations adopting the spherical cavity expansion method. The two-layered soil profiles comprised sands of different relative densities and clays with different undrained shear strengths. Penetration under both drained and undrained conditions was considered. The measured transitions of penetrometer end resistance revealed unexpected differences between penetration in two sand layers and penetration in two clay layers; these differences occurred for both drained and undrained penetration in the clay. The ability of the spherical cavity expansion method to reproduce the experimental trends is investigated, and it has been shown that it is unable to match experimental observations in layered sands.

Keywords: Cone penetration test; layered soil; drainage condition; spherical cavity expansion

1 INTRODUCTION

The Cone Penetration Test (CPT) is widely used in geotechnical practice to delineate site stratigraphy and to assist directly in the design of geotechnical structures. However, the natural variability of the ground, combined with scale effects, poses difficulties in applying direct CPT measurements to evaluate pile end-bearing resistance, as field penetrometers are one or two orders of magnitude smaller than typical piles. This challenge prompted the authors to conduct physical and numerical penetration tests in well-defined layered stratigraphies to improve understanding of the effect of soil layering and penetrometer size.

The contrast of soil stiffness in layered soil profiles has been a focus of different types of numerical simulations. These have employed the Arbitrary Lagrangian-Eulerian (ALE) method (e.g. Walker & Yu 2010), numerical analyses using FLAC with prescribed soil displacements along the axis of symmetry (Ahmadi & Robertson 2005), large deformation Finite Element studies (Ma et al. 2015), the spherical cavity expansion (SCE) method (Xu & Lehane 2008) and others. Amongst these approaches, the SCE method is often employed to study parameters affecting CPT resistance because of its simplicity and efficiency (e.g. Yu & Michell 1998, Mo et al. 2017, Arafianto et al. 2024). Physical tests conducted in calibration chambers and centrifuges provide key insights, but their interpretation is complicated by factors such as shallow penetration effects (Tehrani et al. 2018), boundary clearance (Hird et al. 2003), and non-uniformity issues. Reported tests are relatively limited and do not allow for more generalised conclusions to be drawn. Motivated by the need to assess the relative density of potentially liquefiable thin sand layers, much of the available data in the literature comprises studies with thinly interbedded sand and clay layers (De Lange et al. 2018; Khosravi et al. 2022).

This paper extends the scope of available data and presents results from an investigation conducted in a calibration (pressure) chamber into the influence of soil type and drainage conditions on the transition of the end resistance developed by a cone penetrometer installed in two-layered soil profiles. Data obtained, including measurements of drained and undrained penetration resistance in clay layers, are inspected to assess the influence of penetration rate and drainage conditions. These trends are also examined with results from layered sand to ascertain whether or not there exists a soil-type dependence on the transition length between two soil layers. The ability of the SCE method to reproduce the observed experimental trends is investigated.

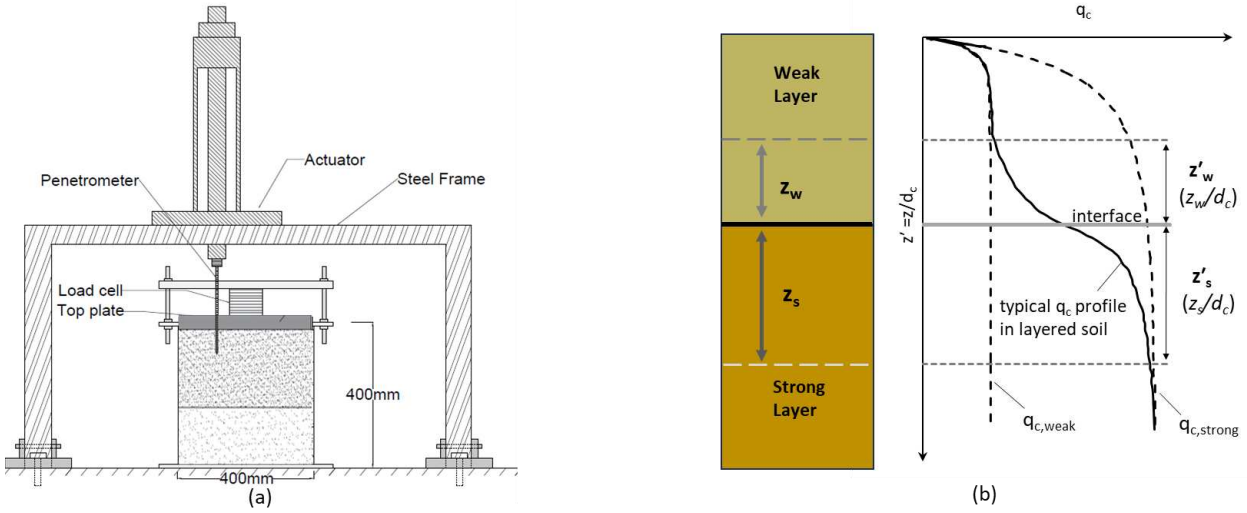

Figure 1. (a) Schematic of the chamber test and (b) terminology for q_c transition in a typical two-layer system

2 TEST PROGRAMME

Cone Penetration Tests (CPTs) were conducted in two-layered soil samples consolidated in a calibration chamber at the University of Western Australia (UWA). The layers comprised various combinations of sand and clay. The sand employed is siliceous and of medium angularity with an average particle size (d_{50}) of 0.18 mm and a uniformity coefficient (C_u) of 1.58. The clay is a commercially sourced Eckaolite kaolin clay with plastic and liquid limits of 44% and 74%, respectively, and a c_v (vertical coefficient of consolidation) of about 7 m^2/year. Both materials have been tested extensively at UWA, with their properties provided in detail by Lehane et al. (2022) and Tian (2025).

2.1 Experimental Procedure

Clay samples were thoroughly mixed at 220% water content until the desired uniform consistency was achieved. The slurry was subsequently transferred into testing chambers and consolidated to the target vertical effective stress. In cases where the sample consisted entirely of clay, one layer was extruded from the chamber and gently positioned over the other layer before the sample was subjected to reconsolidation and penetration.

Sand layers were created by both dry and water pluviation deposited from a sand hopper. A constant horizontal travel speed of the hopper and vertical drop height were maintained within the same layer to ensure sample uniformity. For samples where both layers were of sand, the top surface of the underlying layer was levelled using a vacuum with a custom-designed nozzle.

For samples with a clay and sand combination, the lower layer was prepared (consolidated or pluviated, depending on the material) before the upper layer was water-pluviated or a pre-consolidated clay block was positioned. Full saturation was ensured during the preparation phase before loading was applied to the sample.

2.2 Test Setup

The chamber was placed under the testing frame, as shown in Figure 1(a). Constant vertical stress was applied using a horizontal bar, where the stress level can be adjusted by tightening or untightening the locking nuts above. During penetration, the stress was maintained and monitored by a load cell positioned between the chamber top plate and the horizontal bar. The top plate had circular openings to allow for penetrometer access, driven at a constant speed by the actuator on the steel frame. The chamber walls are rigid and coated with Teflon spray to minimise wall friction.

Miniature penetrometers of 6 mm and 7 mm diameter (d_c) were employed for the reported test series, with a detailed design given in Tian (2025). The corresponding d_c/d_{50} ratios are well over 20 for the sand (Bolton et al. 1999), and the distance between test locations and the boundary exceeds the required minimum clearance of 12 d_c, as reported by Tian and Lehane (2022).

2.3 Definitions

Transition distances are typically used to characterise the variation of q_c transitioning in a two-layered soil system, where z_s and z_w are measured in the strong and

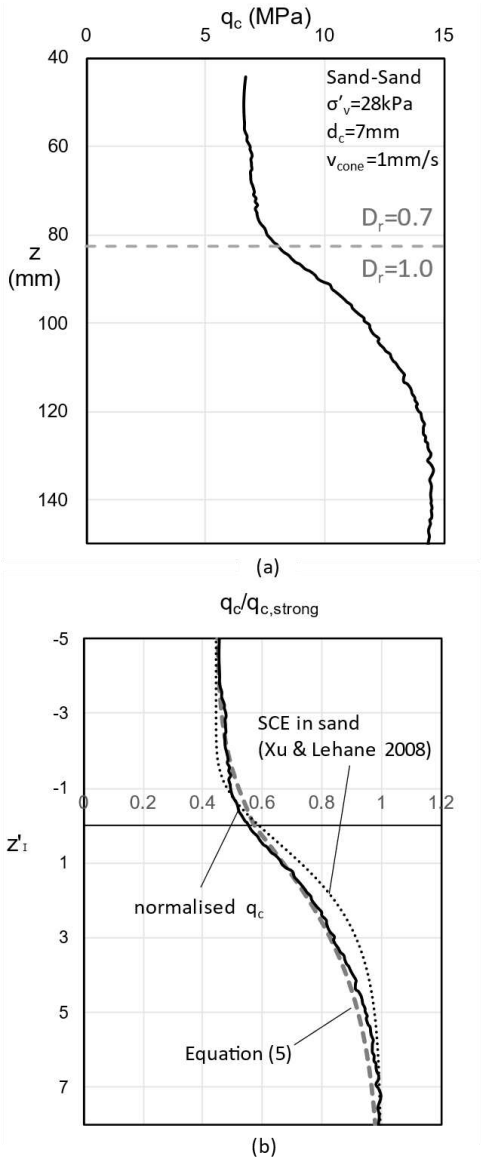

Figure 2. (a) measured q_c profile in layered sand and (b) comparison of q_c curve in normalised form with profiles predicted by Equations (5) and SCE method by Xu & Lehane (2008)

weak layers, respectively. These values are often normalised by the penetrometer diameter (z'_s & z'_w) to enable comparison of q_c profiles obtained by cones of different sizes. The definitions are illustrated schematically in Figure 1(b); note that the relative location of the layers (over or underlying) is inconsequential.

The transition lengths have been reported to have a dependence on r, the ratio of steady-state tip resistance in the two layers, as given below:

$$r = q_{c,weak}/q_{c,strong} \quad (1)$$

where $q_{c,weak}$ and $q_{c,strong}$ are the measured steady-state tip resistance in the weak and strong layers, respectively.

2.4 Experimental Results

2.4.1 Effect of soil type

Drained Penetration in layered sand

Figure 2(a) presents a typical example of q_c measured in a calibration chamber in a two-layered sand stratigraphy consisting of a sand layer with a relative density (D_r) of 0.7 overlying a very dense layer with D_r = 1.0. The cone diameter (d_c) employed was 7 mm, and the applied vertical effective stress (σ'_v) was 28 kPa. It is observed that the measurements stabilise at 7 MPa and 14.6 MPa in the respective layers, indicating that steady-state penetration is reached before the effect of another layer emerges.

The transition length in the upper weaker layer (z_w) is approximately 8 mm ($z'_w \approx 1\ d_c$), and the transition length in the lower stronger layer (z_s) is about 32 mm ($z'_s \approx 5\ d_c$). This result agrees with previously reported observations (Tehrani et al. 2018). Tian & Lehane (2025) have shown that the scale differences of penetrometers in a two-layer system can be offset by adopting the normalised relative depth from the interface, z'_I, defined as follows:

$$z'_I = (z - H_t)/d_c \quad (2)$$

where z (mm) is the penetrometer depth, and H_t (mm) is the thickness of the upper layer.

The reported q_c profile is replotted in the normalised format in Figure 2(b), using $q_c/q_{c,strong}$ and z'_I.

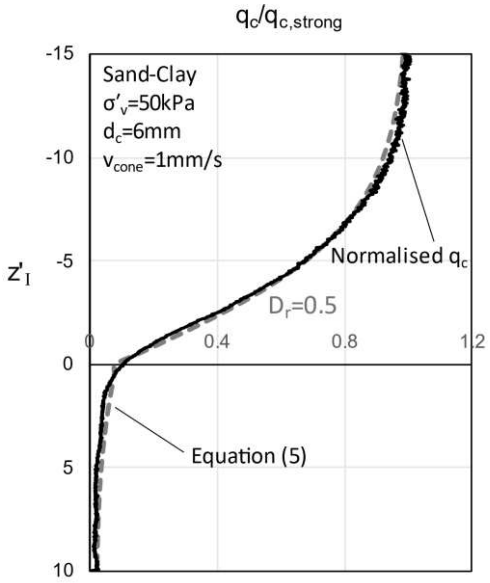

Figure 3. Comparison of normalised CPT curve and predictions by Equations (5) in a sand-clay system.

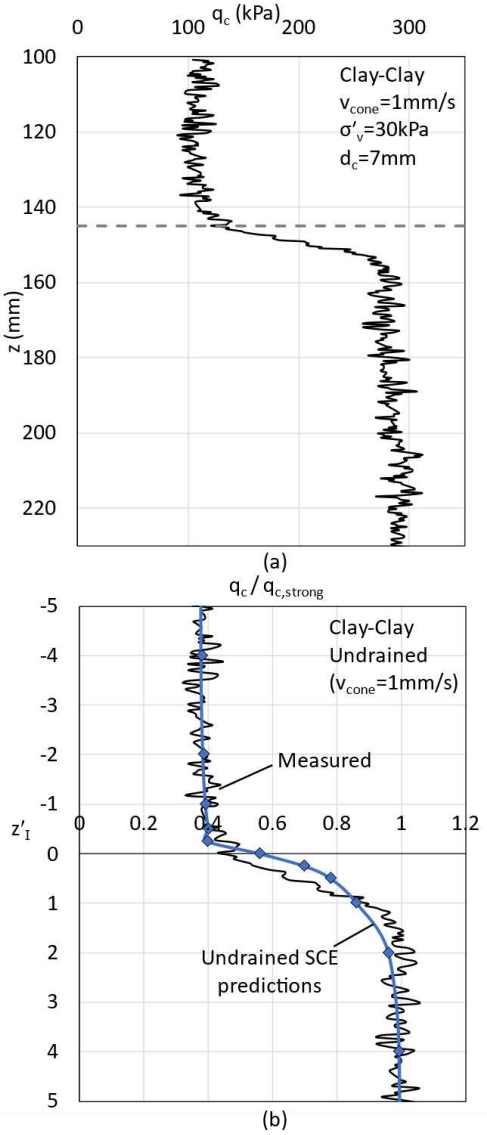

Figure 4. Tip resistance in layered clay (undrained condition): (a) measured value; (b) normalised scale compared with SCE result.

Undrained penetration in layered sand-clay

Figure 3 presents the results of a CPT conducted in a sand-clay sample using a 6mm cone under σ'_v of 50 kPa, where the contrast in layer strengths is high (corresponding to a low r ratio of 0.05). The figure employs normalised axes, where $q_{c,strong}$ is measured to be 5.4 MPa. An increased transition length is observed compared to Figure 2, with z'_s and z'_w values measured to be approximately 13 d_c and 5 d_c, respectively. Post-experiment investigations revealed that a sand-filled conical depression of around 5 d_c depth had formed inside the clay layer. Such an occurrence was also reported by Khosravi et al. (2022) and is likely to have contributed to the observed final length of z'_w. This hypothesis is supported by observations from a separate experiment by the authors using the same r value but where the layer order was reversed. In this case, clay traces were not found in the underlying sand, and a much smaller z'_w value of 1.5 d_c was observed. The value of z'_s remains unchanged for the reversed order of soil layers.

Undrained penetration in layered clay

A typical q_c profile in two-layered clay with σ'_v = 30 kPa is shown in Figure 4(a). The tip resistance was measured at a penetration rate of 1 mm/s, which corresponds to undrained conditions with a normalised velocity (V_v) of 32, defined as (Finnie & Randolph 1994):

$$V_v = v_{cone} \cdot d_c / c_v \quad (3)$$

The transition lengths in both clay layers are evidently much shorter than in sand for a comparable r ratio (see Figure 2). The same undrained penetration data are replotted in normalised form in Figure 4(b). It is seen that $z'_w \approx 0.5\ d_c$ and $z'_s \approx 1.5\ d_c$. These transition lengths are significantly smaller than the respective values at a similar r value of $z'_w \approx 1.3\ d_c$ and $z'_s \approx 5\ d_c$ shown in Figure 2(b).

2.4.2 Effect of drainage condition

A second experiment was performed in the same clay sample employed for the test plotted in Figure 5. However, in this case, a reduced cone velocity of 0.025 mm/s was employed, translating to an equivalent V_v of 0.8; this normalised velocity corresponds to a state approaching drained installation (Suzuki & Lehane 2015).

The q_c curve measured for v_{cone} = 0.025 mm/s is shown in Figure 5(a). Although somewhat surprisingly the cone resistances of the clay have not increased significantly above those shown in Figure 4(a) for undrained penetration, it is evident that the transition length for the undrained and near-drained traces are closely comparable. This similarity is also evident in the normalised plots in Figures 4(b) and 5(b).

3 NUMERICAL ANALYSIS

3.1 Simulation Approach and Procedure

Numerical simulation of the penetration test was conducted in PLAXIS 2D using the spherical cavity expansion (SCE) analogue in layered clay. The nonlinearity of soil stiffness influences the limit pressure (p_{limit}) during the expansion of the cavity. The hardening soil (HS) constitutive model (Schanz et al. 1999) is therefore adopted to account for the soil beha-

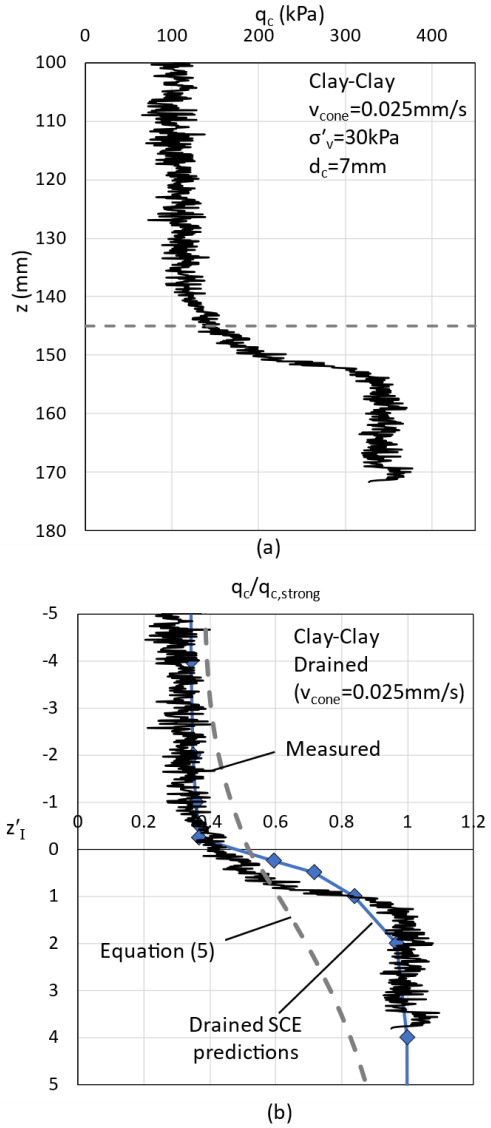

Figure 5. Tip resistance in layered clay (approaching drained conditions, V_v=0.8): (a) measured value; (b) normalised scale compared with predictions by Equations (5) and SCE result.

viour under shear loading and volumetric hardening in cohesive and cohesionless materials.

The SCE results presented here for layered sand were reported by Xu & Lehane (2008), and the same approach for clay is adopted here for ease of comparison. The SCE simulation is conducted by prescribing a positive volumetric strain to a cavity cluster located at the centre of the model, after imposing a constant vertical effective stress on the sample. The cavity, in turn, expands to twice its initial size, either slowly or rapidly, depending on the target drainage condition. The limit pressures (p_{limit}) measured at different depths of the model are used to calculate the tip resistance at corresponding locations in the sand or clay model (Randolph et al. 1994, Suzuki & Lehane 2015), as given in the following equations:

$$q_{c,sand} = p_{limit}[1 + tan\phi' \cdot \tan(45 + \phi'/2)] \quad (4a)$$

$$q_{c,clay} = p_{limit} + \sqrt{3}(p_{limit} - u) \cdot tan\delta \quad (4b)$$

where ϕ' (°) is the peak friction angle of the sand, u is the generated pore pressure due to cavity expansion, and δ (°) is the interface friction angle between soil and cone.

3.2 SCE Simulation Results

Simulation in the two-layered clay adopted a s_u ratio of 1:4 between layers, corresponding to experimental observations. The secant modulus (E_{50}^{ref}) in the two layers was set as 5250 and 21 kPa, respectively, with E equal to $350 \cdot s_u$. The oedometric modulus (E_{oed}^{ref}) was assigned the same value as E_{50}^{ref}, while the modulus exponent (m) was set to 1. The predictions obtained for undrained and drained conditions are compared with experimental data in Figure 4(b) and Figure 5(b). Good agreement between predictions and measurements is obtained and confirm the independence of the transition length on the drainage conditions for the case examined.

SCE predictions for the two-layered sand case (Xu & Lehane) are shown in Figure 2(b). In this case, however, it is seen that the SCE overpredicts the transition length in the denser sand (z'_s). Further analyses reveal that the over-estimation of z'_s by the SCE approach in sands becomes even larger as r decreases and tends to zero.

4 DISCUSSION

A review of the test data highlighted the need for a generalised approach to investigate transition curves in two-layered soil profiles. The formulations proposed by Tian & Lehane (2025), based on test results from sand-sand and sand-clay systems, are adopted to facilitate comparison and are expressed as follows:

$$q_{C\,(w)} = q_{c,0} - tanh[a_W \cdot |z'_I|]\,(q_{c,0} - q_{c,weak}) \quad (5a)$$

$$q_{C\,(s)} = q_{c,0} + tanh[a_S \cdot |z'_I|]\,(q_{c,strong} - q_{c,0}) \quad (5b)$$

where $q_{c(w)}$ is the tip resistance profile in the weak layer, $q_{c(s)}$ is that in the strong and $q_{c,0}$ is the resistance measured at the soil interface. $q_{c,0}$, a_w and a_s are functions of r:

$$a_s = 0.7r^2 + 0.15 \quad (6a)$$

$$a_w = a_s + 0.4r < 1 \quad (6b)$$

$$q_{c,0} = 0.96r^{0.64} \cdot q_{c,strong} \quad (6c)$$

The q_c profiles in layered sand and sand-clay samples determined using Equations (5) are shown in Figures

2(b) and 3, where the formulations evidently provide a good representation of the data recorded in the two samples. However, the same degree of fit is not apparent in the two-layered clay sample due to the shorter transition lengths observed in Figure 5. A similar difference in transition lengths between layered sand and layered clay was observed in the test series reported by Hird et al. (2003) and Liu et al. (2020). LDFE analysis conducted by Ma et al. (2015) has also displayed a shorter transition in layered clay compared to the typical values obtained in layered sand. Further study is required to examine this phenomenon more closely.

Preliminary investigations have highlighted significant differences between using the (simple) SCE approach and more sophisticated full-flow analyses to model penetrometer installation. Arafianto and Lehane (2025) present results adopting the press-replace method (PRM) for penetrometer installation in two-layered samples. These results were successful in replicating the trends indicated in Figures 2 through 5. Therefore, the SCE approach is not recommended for further study of the influence of layering on penetrometer resistance.

5 CONCLUSIONS

Experimental and numerical investigations of the transition of penetrometer end resistance in two-layered samples have shown:

1. The transition length of penetrometer resistance in two-layered clay profiles is shorter than in two sand layers.
2. The transition length during undrained and drained penetration in clay is approximately the same.
3. The Spherical Cavity Expansion (SCE) approach provides reasonable predictions for the transition of drained and undrained penetrometer end resistance in clay.
4. The SCE approach underestimates the transition length in a two-layered sand sample; this is attributed to deficiencies in the SCE approach, which can be overcome by modelling the 2D nature of penetrometer installation, as shown by the preliminary findings of this study.

AUTHOR CONTRIBUTION STATEMENT

Y. Tian: Conceptualization, Methodology, Investigation, Data Curation, Formal Analysis, Writing- Original Draft; Reviewing and Editing. **A. Arafianto**: Numerical investigations, Writing- Original Draft; Reviewing and Editing. **B. M. Lehane**: Supervision, Funding acquisition, Conceptualization, Methodology, Writing- Reviewing and Editing.

ACKNOWLEDGEMENT

The first author is grateful for the financial support of the Research Training Program (RTP) scholarship from the Australian government.

The second author acknowledges the support from Universitas Katolik Parahyangan, the PhD scholarship from the Ministry of Finance of Indonesia, and the ARC Linkage Project HDR Top-Up Scholarship from the University of Western Australia.

REFERENCES

Ahmadi, M.M. and Robertson, P.K. (2005). Thin-layer effects on the CPT q_c measurement. *Canadian Geotechnical Journal,* 42(5), pp.1302-1317.

Arafianto, A., and Lehane, B. M. (2025). Interpretation of CPT End Resistance in a Two-Layered Soil System using Finite Element Method, [Submitted to Acta Geotechnica].

Arafianto, A., Tian, Y., Lehane, B.M., Suzuki, Y. and Reid, D., (2024). Experimental and numerical investigations of CPT end resistance at variable penetration rates in mixed soils. In *ISC2024*.

Bolton, M.D., Gui, M.W., Garnier, J., Corte, J.F., Bagge, G., Laue, J., and Renzi, R. (1999). Centrifuge cone penetration tests in sand. *Géotechnique,* 49(4): 543-552, doi.org/10.1680/geot.1999.49.4.543

De Lange, D.A, Terwindt, J. and van der Linden T.I. (2018). CPT in thinly inter-layered soils. In *Cone Penetration Testing 2018*, pp. 383-388.

Finnie, I.M.S. and Randolph, M.F. (1994). Punch-through and liquefaction induced failure of shallow foundations on calcareous sediments. In *Proceedings of the 17th International Conference on the Behaviour of Offshore Structures (BOSS'94)*, Boston, MA, USA (Chryssostomidis C (ed)).

Hird, C.C., Johnson, P. and Sills, G.C. (2003). Performance of miniature piezocones in thinly layered soils. *Geotechnique,* 53(10), pp.885-900.

Khosravi, M., DeJong, J.T., Boulanger, R.W., Khosravi, A., Hajialilue-Bonab, M., Sinha, S.K. and Wilson, D. (2022). Centrifuge tests of cone-penetration test of layered soil. *Journal of Geotechnical and Geoenvironmental Engineering*, 148(4), p.04022002.

Lehane, B.M., Zania, V., Chow, S.H. and Jensen, M. (2022). Interpretation of centrifuge CPT data in normally consolidated silica and carbonate sands. *Géotechnique*, pp.1-10.

Liu, Q.B., Lehane, B.M. and Tian, Y. (2020). Bearing capacity and stiffness of embedded circular footings on stiff-over-soft clay. *Journal of Geotechnical and Geoenvironmental Engineering*, 146(11), 06020020. doi.org/10.1061/(ASCE)GT.1943-5606.0002393

Ma, H., Zhou, M., Hu, Y. & Shazzad Hossain, M. (2015). Interpretation of layer boundaries and shear strengths for soft-stiff-soft clays using CPT data: LDFE analyses. *Journal of Geotechnical and Geoenvironmental Engineering*, 142(1), 04015055. doi.org/10.1061/(ASCE)GT.1943-5606.000137

Mo, P.Q., Marshall, A.M., and Yu, H.S. (2017). Interpretation of Cone Penetration Test Data in Layered Soils Using Cavity Expansion Analysis. *Journal of Geotechnical and Geoenvironmental Engineering*, 143(1): 04016084. doi:10.1061/(ASCE)GT.1943-5606.0001577.

Randolph, M.F., Dolwin, J. and Beck, R. (1994). Design of driven piles in sand. *Géotechnique*, 44(3), pp427-448.

Schanz, T., Vermeer, P.A., and Bonnier, P.G. (1999). The hardening soil model: Formulation and verification. In *Beyond 2000 in Computational Geotechnics*.

Suzuki, Y., and Lehane, B.M. (2015). Analysis of CPT end resistance at variable penetration rates using the spherical cavity expansion method in normally consolidated soils. *Comp Geot*, 69: 141-152.

Tehrani, F.S., Arshad, M.I., Prezzi, M. and Salgado, R. (2018). Physical modeling of cone penetration in layered sand. *Journal of Geotechnical and Geoenvironmental Engineering*, 144(1), p.04017101.

Tian. Y. (2025). Investigation of CPT response in uniform and layered soil. PhD Thesis, Dept. Civil, Environmental and Mining Engineering, Univ. of Western Australia.

Tian, Y. and Lehane, B.M. (2022). Parameters affecting the CPT resistance of reconstituted sands. In *Cone Penetration Testing 2022,* pp. 734-740. CRC Press.

Tian, Y. and Lehane, B.M. (2025). The influence of soil layering and penetrometer diameter on penetration resistance. *Canadian Geotechnical Journal*.

Walker, J. and Yu, H. S. (2010). Analysis of the cone penetration test in layered clay. *Géotechnique,* 60(12), pp. 939–948.

Xu, X. and Lehane, B.M. (2008). Pile and penetrometer end bearing resistance in two-layered soil profiles. *Géotechnique*, 58(3), pp.187-197.

Yu, H.S., and Mitchell, J.K. (1998). Analysis of Cone Resistance: Review of Methods. *Journal of Geotechnical and Geoenvironmental Engineering*, 124(2): 140-149. doi:10.1061/(ASCE)1090-0241(1998)124:2(140).